

Electronic and magnetic properties of zigzag graphene nanoribbons on the (111) surface of Cu, Ag and Au

Yan Li¹, Wei Zhang¹, Markus Morgenstern², and Riccardo Mazzarello^{1*}

¹ *Institute for Theoretical Solid State Physics and JARA,
RWTH Aachen University, D-52074 Aachen, Germany*

² *II. Physikalisches Institut B and JARA-FIT, RWTH Aachen University, D-52074 Aachen, Germany*
(Dated: October 11, 2012)

We have carried out an *ab initio* study of the structural, electronic and magnetic properties of zigzag graphene nanoribbons on Cu(111), Ag(111) and Au(111). Both, H-free and H-terminated nanoribbons are considered revealing that the nanoribbons invariably possess edge states when deposited on these surfaces. In spite of this, they do not exhibit a significant magnetization at the edge, with the exception of H-terminated nanoribbons on Au(111), whose zero-temperature magnetic properties are comparable to those of free-standing nanoribbons. These results are explained by the different hybridization between the graphene 2p orbitals and those of the substrates and, for some models, by the sizable charge transfer between the surface and the nanoribbon. Interestingly, H-free nanoribbons on Au(111) and Ag(111) exhibit two main peaks in the local density of states around the Fermi energy, which originate from different states and, thus, do not indicate edge magnetism.

PACS numbers:

Graphene [1] with its remarkable electronic and transport properties [2], in particular a high room-temperature mobility [3], is a promising material for applications in information technology. While perfect monolayer graphene has a gapless spectrum prohibiting standard transistor applications, nanostructuring can induce the required band gap. Recent efforts focused on quasi one-dimensional graphene nanoribbons (GNRs) [4–7] and zero-dimensional graphene quantum dots (GQDs) [8–10] and, indeed, revealed a transport gap, e.g. for GNRs with widths below 10 nm. Theoretically, unsupported GNRs and GQDs with zigzag edge geometry possess spin polarized edge states with ferromagnetic order along the edge [11–13]. Several experimental studies provide direct [10, 14–16] or indirect [17] evidence for the presence of the edge states also in supported GNRs, albeit without probing its magnetism. Such edge states might be exploited for a multitude of spintronics applications [4, 18–20], but so far it is unclear, if the edge states contribute to the measured transport properties of nanostructures at all. Thus, it is important to elucidate the role of the substrate and of edge termination.

Recently, several groups including us investigated in-situ prepared GQDs with exclusive zig-zag-edges, which are supported by Ir(111) [21–27]. In particular, we revealed the absence of edge states by a combined Density Functional Theory (DFT) and scanning tunneling microscopy (STM) study [28]. Our finding was explained by a hybridization of the graphene π -orbitals with an Ir $5d_{z^2}$ surface state at E_F , which gradually decreases in strength from the edge towards the center of the GQD and, thus, prohibits a simple shift of the edge state towards the interior of the GQD [28]. In contrast, STM studies of Tao *et al.* [16] provided convincing evidence for the presence of edge states in GNRs chemically prepared

from carbon nanotubes by so called unzipping [29] and deposited on Au(111). A peak or a double-peak close to E_F was observed in the local density of states (DOS) close to the edge with a peak distance scaling with the width of the GNR. The double-peak was present for chiral angles θ up to 16.1° with respect to the zigzag direction and was ascribed to an antiferromagnetic coupling between opposite edges [16, 30] as further evidenced by comparison with results from a Hubbard model Hamiltonian [16].

Here, we present a more realistic description of this system using DFT and including the Au(111) surface. Large models were used, which enabled us to study GNRs of close to realistic widths and to correctly describe the lattice mismatch between graphene and Au(111). For comparison, we also investigated GNRs deposited on the (111) surface of the other two group 1B metals, Cu and Ag. For all the substrates, we considered both H-free and singly H-terminated GNRs. For H-free GNRs on Au(111), which is most relevant to the experiments by Tao *et al.* [16], we considered the two chiral angles $\theta = 0^\circ$ and 5° , while only perfect zigzag GNRs were studied for the other systems. We show that all the GNRs studied exhibit edge states, but that the interaction with the substrate strongly depends on whether the GNR is H-terminated or not and, to a lesser extent, also on the type of substrate. As a result, it turns out that the edge states are magnetic only when H-terminated and deposited on Au(111). Exactly this system was prepared experimentally recently [29, 31]. Interestingly, the nonmagnetic H-free GNR on Au(111) also exhibits a double peak around E_F (albeit with a much larger splitting as compared to experiments [16]), but the two peaks originate from a hybridization of Au d-orbitals with the graphene and the unoccupied edge state, respectively, and not from a magnetic splitting of

	H-free GNR		H-terminated GNR	
	min	max	min	max
Cu	1.96	3.31	2.37	3.06
Ag	2.18	5.61	2.69	3.16
Au	2.12	5.75	3.45	3.48

TABLE I: Minimum distance between the edge C atoms of the GNR and the atoms of the relevant (111) surface and maximum distance between the center of the GNR and the surface. Distances are in Angstrom.

the edge state.

We considered GNRs with zigzag edges and a width of 8 graphene unit cells. We employed different supercells in order to account for a) the lattice mismatch between graphene and the (111) surfaces of Cu, Ag and Au and b) chiral angles. Here, we describe the models having $\theta = 0^\circ$ (the model with finite θ is discussed in the Supplement [32]). For Ag and Au a supercell with a size parallel to the GNR six times as large as the unit cell of the (111) surface was used. For Cu, an extremely large supercell would be required to account for the mismatch, making the calculations unfeasible. Therefore, a slightly compressed (about 3.8 %) Cu lattice was instead used to make graphene and Cu(111) commensurate. A four-layer slab was used for Ag and Au surfaces, whereas the use of a smaller supercell for Cu (in the direction parallel to the GNR) enabled us to employ thicker slabs containing up to 12 layers. The latter calculations showed that 4-layer slabs are sufficient to describe semi-quantitatively the interaction between the GNR and the Cu surface (see Supplement), making us confident that the same holds true for Ag and Au substrates.

The structural optimization and the calculation of the electronic and magnetic properties were carried out using the plane-wave package Quantum-Espresso [33]. Additional computational details are provided in the Supplement [32].

In the first part of the paper, we present our results about the GNRs on Au(111). Ag and Au substrates are discussed in the second part and in the Supplement [32]. Upon DFT relaxation, the H-free GNR with $\theta = 0^\circ$ on Au(111) bends considerably: the distance between C atoms and the surface is much shorter at the GNR edge than in the interior of the ribbon (Fig. 1(a)). The maximum distance between C atoms and the Au (as well as Cu and Ag) surface at the center of the GNR and the minimum distance at the edge are shown in Table I. A small corrugation (about 0.17 Å) along the GNR edges in accordance with the Moiré periodicity is observed. In particular, 4 edge C atoms out of 7 are in a quasi on-top configuration, whereas the remaining edge atoms are in a quasi bridge or hollow configuration. In the following, the z axis will be taken perpendicular to the surface and the x axis will be taken parallel to the GNR. Since the

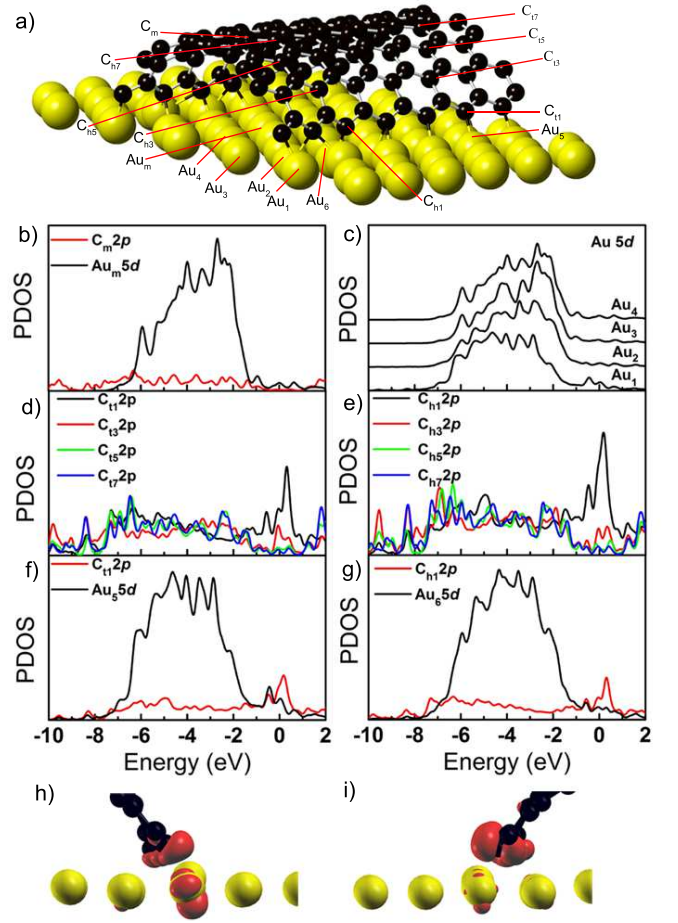


FIG. 1: Structural and electronic properties of a H-free GNR on Au(111). (a) Topography of the relaxed model. For the sake of clarity, only the top Au layer is shown. C and Au atoms are labeled by numbers indicating different chemical environments and used in (b)-(g). The top and hollow adsorption sites of the edge C atoms are denoted with the subscripts “t” and “h” respectively. (b) $(p_y + p_z)$ -PDOS of a C atom (C_m) in the middle part of the GNR and PDOS of the d states of an Au atom (Au_m) located beneath. (c) PDOS of d states of several Au atoms starting from an atom below the edge of the GNR (Au_1) towards an atom below the centre of the GNR (Au_4). (d), (e) $(p_y + p_z)$ -PDOS of C atoms at the center of the on-top (d) and hollow (e) region, in increasing distance from the edges; row 1 denotes the edge row. (f), (g) $(p_y + p_z)$ -PDOS of an edge C atom at on-top site, C_{t1} (f), and at hollow site, C_{h1} (g), and PDOS of the d states of the nearest neighbor Au atom (Au_5 and Au_6 respectively). (h), (i) Plots of a charge isosurface of a state contributing to the peak at -0.2 eV below E_F (h) and at 0.3 eV above E_F (i).

GNR is not parallel to the surface at the edge, the orbitals of C forming edge states are linear combination of $2p_z$ and $2p_y$ orbitals. For the same reason, the dangling-bond orbitals of the edge C atoms of the H-free GNR (which form σ bonds with Au atoms upon deposition on the surface, see below) are also combinations of these or-

bitals. In Fig. 1(b) the $(p_y + p_z)$ -PDOS of a C atom in the middle part of the GNR and the PDOS of the 5d states of an Au atom located beneath are shown: the contribution of the PDOS of the d states of Au near E_F is very small and the interaction between the two atoms is basically negligible. On the other hand, a comparison of the PDOS of the d states of several Au atoms starting from an Au atom below the edge of the GNR towards an Au atom below the centre (Fig. 1(c)) shows that, at the edge, the PDOS displays some peaks near E_F . Also, the $(p_y + p_z)$ -PDOS of the edge C atoms (Figs. 1(d)-(e)) exhibit two main peaks near E_F . To shed light on the interaction between edge C atoms and Au atoms, it is useful to compare the respective PDOS at on-top sites (Fig. 1(f)) and hollow sites (Fig. 1(g)). The $(p_y + p_z)$ -PDOS of a C atom at an on-top site displays two peaks at -0.2 eV below and 0.3 eV above E_F respectively. Inspection of the PDOS of the nearest neighbor Au 5d orbitals indicates that a strong hybridization between these states and C states occurs. In particular, a relatively high peak below E_F is present, in correspondence with the small peak of the C p states, whereas a less pronounced peak is found right above E_F , corresponding to the second, large peak of the C p PDOS. In the hollow case, two peaks are present in the PDOS of C p states as well, whereas the PDOS of the nearest neighbor Au d states exhibits no peak above E_F . These findings suggest that the two peaks in the PDOS of C p orbitals near E_F have a different origin. In fact, the plots of charge isosurfaces of two states contributing to said peaks (Figs. 1(h)-(i)) unequivocally show that the one above E_F is due to the π edge states of the GNR, whereas the one below E_F is due to states originating from σ bonding between C and Au atoms. More precisely, the latter peak corresponds to antibonding p-d states, whereas the corresponding bonding states have much lower energies (about -5 eV below E_F). In the on-top case, the $5d_{z^2}$ and $5d_{yz}$ orbitals of the Au mostly contribute to the bonding with C p states; in the hollow case, $5d_{zx}$ orbitals contribute as well. Au 6s and 6p orbitals do not play an important role in this bonding. Since the antibonding σ states have lower energies than the edge states, the latter states are mostly unoccupied and no significant edge magnetism occurs (less than $3 \cdot 10^{-3} \mu_B$ per edge C atom).

The model of the GNR with $\theta = 5^\circ$ is presented in the Supplement. This model also bends considerably and exhibits essentially non-magnetic edge states for similar reasons (see Fig. S1).

Next, we consider H-terminated GNRs on Au(111). In this case, the interaction between the GNR and the surface is weak: the minimum distance between the edge C atoms and the surface is 3.45 Å (see Table I). The GNR is almost flat, as evident from Figs. 2(a)-(b). As a result, the electronic properties of the GNR are weakly affected by the presence of the substrate: the GNR displays a magnetic edge state with antiferromagnetic cou-

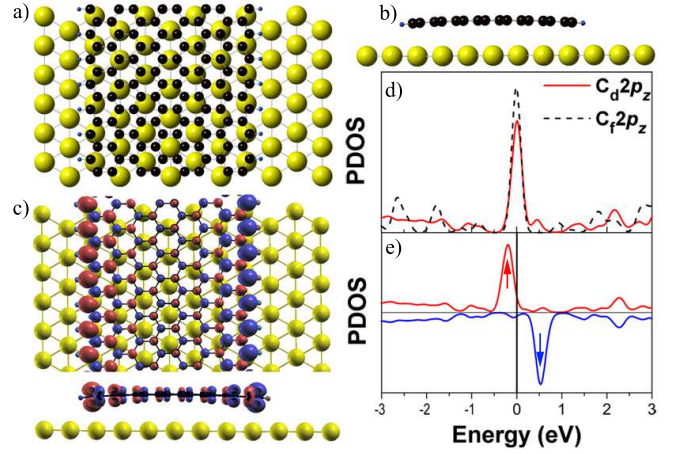


FIG. 2: Structural and electronic properties of a H-terminated GNR on Au(111). (a)-(b) Top and side view of the relaxed model. Only the top Au layer is shown. (c) Top and side view of an isovalue surface of the edge state spin density of the deposited GNR. The system has antiferromagnetic order across the GNR. The red (blue) surface indicates spin up (down) density. (d) Non-spin-polarized PDOS of the $2p_z$ orbitals of an edge C atom of the deposited GNR (C_d). The corresponding PDOS of the edge C atom of the free-standing GNR (C_f) is also shown for comparison. (e) Spin-polarized PDOS of the $2p_z$ orbitals of a C atom at the left edge of the magnetized GNR shown in Fig. (c).

pling between the edges and the magnetization per edge C atom is about $0.22 \mu_B$ (comparable to the value obtained for free-standing GNRs using equivalent k-point meshes, see Supplement). An isovalue surface of the edge state spin density is shown in Fig. 2(c), whereas the spin-unpolarized and spin-polarized PDOS of the $2p_z$ orbitals of edge C atoms are shown in Figs. 2(d) and (e) respectively. The energy splitting between spin majority and minority $2p_z$ peaks on an edge is about 0.7 eV (Fig. 2(e)).

Since the edges of the GNRs investigated experimentally in Ref. 16 exhibit a pronounced edge curvature, they resemble the H-free case of our calculation. A comparison of the experimentally observed peak splitting with the calculated one is tempting, although the experimental GNR width of 8 nm to 20 nm is much larger than in our models (1.6 nm). The experimentally observed energy difference ranges from 50 meV to 20 meV [16] and is an order of magnitude lower than the one from the DFT calculation. Thus, a direct assignment of the calculated splitting to the experimental results is not possible, maybe due to a different edge chemistry, but our findings suggest that the interpretation of a double peak around E_F alone as a sign for edge magnetism might be misleading.

Naively, one could expect that the properties of the GNRs on Ag(111) would be almost identical to those discussed above. Indeed the electronic structure of H-free

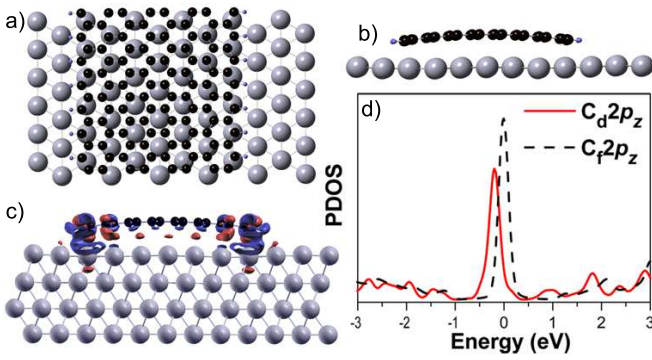


FIG. 3: Structural and electronic properties of a H-terminated GNR on Ag(111). (a)-(b) Top and side view of the relaxed model. Only the top Ag layer is shown. (c) Isovalue surfaces of the difference between the total charge of the GNR plus substrate system and the charge of the isolated (bent) GNR and Ag(111). The red (blue) color indicates accumulation (depletion) of charge. (d) PDOS of the $2p_z$ orbitals of an edge C atom of the deposited GNR (C_d). The non-spin-polarized $2p_z$ PDOS of the edge C atom of the free-standing GNR (C_f) is also shown.

GNRs on Ag(111) is qualitatively similar to that of the nanoribbons deposited on Au, as discussed in the Supplement. On the other hand, H-terminated GNRs on Ag(111) exhibit remarkable differences with respect to Au(111), which originate from the relatively strong interaction between the GNRs and the Ag substrate. In fact, the minimum distance between the C atoms and Ag(111) is 2.69 \AA at the edge (Table I) and a significant bending of the GNR occurs (Figs. 3(a)-(b)). The interaction between Ag atoms and edge C atoms is partly covalent and a net charge transfer from the surface to the GNR also occurs, as evident from Fig. 3(c). In total, the GNR has acquired a charge of $1.6 \cdot 10^{-2}$ electrons per C atoms. This behavior is in contrast to the case of Au(111) and can be qualitatively explained by the fact that Ag is more prone to donate electrons than Au. The PDOS of the C $2p_z$ orbitals exhibits a large peak (Fig. 3(d)), which corresponds to the edge states. However, due to the n doping of the GNR, the peak is not exactly at E_F but is shifted slightly downwards in energy. As a result, the DOS at E_F is small and no Stoner instability occurs: hence, this system is non magnetic. In fact, the calculated magnetization is less than $10^{-3} \mu_B$ per edge C atom. Furthermore, the height of the PDOS peak is also reduced with respect to the free-standing case, due to the interaction with the Ag atoms (Fig. 3(d)).

GNRs on Cu(111) display significant structural differences with respect to the Au and Ag substrate, which stem from the stronger reactivity of Cu atoms. In particular, in the H-free case, the interaction between the GNR and the Cu substrate is not negligible even in the center of the GNR and the maximum distance between

the latter and the surface is only 3.31 \AA (see Table I and Fig. S2a). The edge state interacts more strongly with the Cu substrate than with Au(111) and Ag(111): nevertheless, the PDOS bears a qualitative resemblance to that of the latter models (see Supplement). In the H-terminated case, the strong interaction between C and Cu atoms also leads to shorter equilibrium distances between the GNR and the substrate (Table I and Figs. S5(a)-(b)). Charge transfer leads to the filling of the edge state in this model too, which is thereby non-magnetic (Figs. S5(c)-(d)).

In conclusion, our simulations based on DFT indicate that zigzag GNRs deposited on Cu(111), Ag(111) and Au(111) all possess edge states but do not exhibit significant edge magnetism, with the exception of H-terminated GNRs on Au(111), whose zero-temperature magnetization is comparable to that of free-standing GNRs. These results are explained by the different interaction and charge transfer between the GNRs and the substrates. Only in the case of H-terminated GNRs on Au(111) is the interaction sufficiently weak so as not to affect the electronic and magnetic properties of the edge states significantly. Hence, our simulations strongly suggest that experimental investigations on edge magnetism in GNRs deposited on metallic substrates should focus on the latter system.

We acknowledge discussions with G. Bihlmayer, C. Honerkamp, M. Schmidt and S. Wessel, the computational resources by the RWTH Rechenzentrum as well as financial support by the DFG via Li 1050/2-1 and Mo 858/8-2.

* Electronic address: mazzarello@physik.rwth-aachen.de

- [1] K. S. Novoselov, A. K. Geim, S. V. Morozov, D. Jiang, Y. Zhang, S. V. Dubonos, I. V. Grigorieva, and A. A. Firsov, *Science* **306**, 666 (2004).
- [2] A. H. Castro Neto, F. Guinea, N. M. R. Peres, K. S. Novoselov, and A. K. Geim, *Rev. Mod. Phys.* **81**, 109 (2009).
- [3] S. V. Morozov, K. S. Novoselov, M. I. Katsnelson, F. Schedin, D. C. Elias, J. A. Jaszczak, and A. K. Geim, *Phys. Rev. Lett.* **100**, 016602 (2008).
- [4] Y. Son, M. L. Cohen, and S. G. Louie, *Nature* **444**, 347 (2006).
- [5] L. Jiao, L. Zhang, X. Wang, G. Diankov, and H. Dai, *Nature* **458**, 877 (2009).
- [6] J. Cai *et al.*, *Nature* **466**, 470 (2010).
- [7] X. Li, X. Wang, L. Zhang, S. Lee, and H. Dai, *Science* **319**, 1229 (2008).
- [8] L. A. Ponomarenko, F. Schedin, M. I. Katsnelson, R. Yang, E. W. Hill, K. S. Novoselov, and A. K. Geim, *Science* **320**, 356 (2008).
- [9] F. Molitor, S. Dröschner, J. Güttinger, A. Jacobsen, C. Stampfer, T. Ihn, and K. Ensslin, *Appl. Phys. Lett.* **94**, 222107 (2009).
- [10] K. A. Ritter and J. W. Lyding, *Nature Mater.* **8**, 235

- (2009).
- [11] M. Fujita, K. Wakabayashi, K. Nakada, and K. Kusakabe, *J. Phys. Soc. Jpn.* **65**, 1920 (1996).
 - [12] K. Nakada, M. Fujita, G. Dresselhaus, and M. S. Dresselhaus, *Phys. Rev. B* **54**, 17954 (1996).
 - [13] T. Wassmann, A. P. Seitsonen, A. M. Saitta, M. Lazzeri, and F. Mauri, *J. Am. Chem. Soc.* **132**, 3440 (2010).
 - [14] Z. Klusek *et al.*, *Appl. Surf. Sci.* **252**, 1221 (2005).
 - [15] M. Pan, E. Costa Girao, X. Jia, S. Bhaviripudi, Q. Li, J. Kong, V. Meunier, and M. S. Dresselhaus, *Nano Lett.* **12**, 1928 (2012).
 - [16] C. Tao *et al.*, *Nature Phys.* **7**, 616 (2011).
 - [17] J. Chae *et al.*, *Nano Lett.* **12**, 1839 (2012).
 - [18] W. Y. Kim and K. S. Kim, *Nature Nanotechnol.* **3**, 408 (2008).
 - [19] K. Wakabayashi, *Phys. Rev. B* **64**, 125428 (2001).
 - [20] M. Wimmer, I. Adagideli, S. Berber, D. Tománek, and K. Richter, *Phys. Rev. Lett.* **100**, 177207 (2008).
 - [21] D. Subramaniam *et al.*, *Phys. Rev. Lett.* **108**, 046801 (2012).
 - [22] P. Lacovig, M. Pozzo, D. Alfè, P. Vilmercati, A. Baraldi, and S. Lizzit, *Phys. Rev. Lett.* **103**, 166101 (2009).
 - [23] S. K. Hämäläinen, Z. Sun, M. P. Boneschanscher, A. Upstu, M. Ijäs, A. Harju, D. Vanmaekelbergh, and P. Liljeroth, *Phys. Rev. Lett.* **107**, 236803 (2011).
 - [24] S.-H. Phark, J. Borme, A. L. Vanegas, M. Corbetta, D. Sander, and J. Kirschner, *Phys. Rev. B* **86**, 045442 (2012).
 - [25] S. J. Altenburg, J. Kröger, T. O. Wehling, B. Sachs, A. I. Lichtenstein, and R. Berndt, *Phys. Rev. Lett.* **108**, 206805 (2012).
 - [26] I. Pletikosić, M. Kralj, P. Pervan, R. Brako, J. Coraux, A. T. N'Diaye, C. Busse, and T. Michely, *Phys. Rev. Lett.* **102**, 056808 (2009).
 - [27] C. Busse *et al.*, *Phys. Rev. Lett.* **107**, 036101 (2011).
 - [28] Y. Li *et al.* (submitted).
 - [29] L. Y. Jiao, X. R. Wang, G. Dyankov, H. L. Wang, and H. Y. Dai, *Nature Nanotechnol.* **5**, 321 (2010).
 - [30] H. Feldner, Z. Y. Meng, T. C. Lang, F. F. Assaad, S. Wessel, and A. Honecker, *Phys. Rev. Lett.* **106**, 226401 (2011).
 - [31] X. Zhang *et al.*, *arXiv* 1205.3516 (2012).
 - [32] see supplementary information at ...
 - [33] P. Giannozzi *et al.*, *J. Phys.: Condens. Matter* **21**, 395502 (2009); <http://www.quantum-espresso.org>.